Regardless of mechanism of photolysis of dichloride 7, this is the precursor of choice for generating *m*-xylene in liquid or solid solution.

Conclusions

Photolysis of polymethylbenzenes can produce *m*-xylylene type biradicals. The mechanism involves the secondary photolysis of the polymethylbenzene triplet state which cleaves a benzylic carbon–hydrogen bond. The nascent hydrogen atom produced can then abstract a second benzylic hydrogen from a nearby methyl group to produce the biradical and molecular hydrogen.

A liquid solution phase fluorescence spectrum of *m*-xylylene is produced by 249 nm laser photolysis of dichloride 7. The mechanism of biradical formation from dichloride 7 is not known.

Experimental Section

Mesitylene (gold label), α,α'-dibromo-*m*-xylene, α,α'-dichloro-*m*-xylene, 2-methylbutane, methylcyclohexane, *n*-hexane, *n*-hexane-d_{14}, ethanol, ethanol-d_6, and 3-methylpentane were purchased from Aldrich Chemical Co. (spectral or HPLC grade where available) and used without further purification. Durene (technical grade) was purchased from Humble Oil and Refining Co. and purified by elution through neutral alumina (hexanes as eluent) immediately prior to preparation of a sample tube. 2-Methyltetrahydrofuran (Aldrich) was refluxed over $KMnO_4$, distilled, and stored over molecular sieves prior to use.

Synthesis of *m*-Tolylacetyl Peroxide (4). *m*-Tolylacetic acid (3.0 g, 19.9 mmol) was treated with thionyl chloride (10 mL), and the resulting solution was heated to reflux (4.5 h). Removal of thionyl chloride by azeotropic distillation with benzene gave *m*-tolylacetyl chloride which was used immediately without further purification. The acid chloride was taken up in 5 mL of tetrahydrofuran. A solution of sodium peroxide (1 g, 0.013 mol) in 10 mL of water was added to the cold stirred solution of the acid chloride. After 1.5 h, the mixture was extracted with diethyl ether. The ether layer was washed with 10% aqueous bicarbonate solution, dried, and removed in vacuo to yield a pale yellow oil (2.1 g; 35%) which tested positive for a peroxide (KI and starch paper). IR: 1800 and 1730 cm^{-1}.

All matrix fluorescence spectra were obtained on a commercial (Perkin-Elmer Model LS-5) spectrofluorimeter. The sample compartment of the LS-5 has been modified so that fluorescence spectra can be recorded on samples in a Dewar flask at the temperature of boiling liquid N_2. Samples were prepared by transferring approximately 0.5 mL of the desired solution into a quartz tube (4 mm o.d.). The samples were then degassed by multiple freeze–pump–thaw cycles prior to sealing under vacuum. Following preparation, we stored samples which were not used immediately at liquid nitrogen temperature until they could be photolyzed and subsequently analyzed.

LIF experiments were performed by using a laser flash photolysis apparatus similar to that described by Scaiano.[14] Briefly, a degassed solution of the precursor having an optical density of ~1.0 at the 249 nm laser line is prepared in a Suprasil quartz sample cuvette. The focussed output of a Lumonics Model TE-860-4 laser impinges upon the sample cell. This laser pulse serves both to dissociate the precursor molecules, forming the reactive radicals and/or biradicals, as well as to promote these reactive species to an electronically excited state. At a 90° angle to this excitation source, the total fluorescence of the sample is monitored. This emitted light is led via a fiber optics cable through a slit (25 μm) onto an Allied analytical systems spectrograph which serves to disperse the fluorescence. The dispersed fluorescence is then collected using a PARC optical multichannel analyzer (OMA) as the detector. The OMA is gated to coincide with the laser pulse. Extraneous scattered laser light is removed by the use of an Oriel 295 nm long pass glass filter placed between the sample compartment and the fiber optics cable.

For the matrix experiments, samples were irradiated at 77 K in a Dewar flask (quartz windows) with the unfocussed output of either a Lumonics Model TE-860-4 excimer laser (KrF; 249 nm, 10 ns pulse, ~80 mJ per pulse), a Molectron N_2 laser (337 nm, 8 mJ per pulse), or a Rayonet Reactor (5 bulbs PRP 254) or a 1000-W Hg–Xe arc lamp as indicated. The intensity of the laser was varied by the use of wire mesh neutral density filters. The absorbance of the filters was monitored prior to and following irradiation to ensure that the filter was not altered by exposure to the intense excimer laser radiation. Reproducible positioning of the Dewar flask in the excimer beam was achieved by mounting a holder on an optical table, so that the sample, in the Dewar flask, could be reproducibly placed in the path of the laser beam.

Acknowledgment. The authors are indebted to the NSF international program and the CNRS for support of this work.

Registry No. 1, 108-67-8; **2**, 19121-63-2; **3**, 57384-02-8; **4**, 123883-43-2; **7**, 626-16-4.

(14) Scaiano, J. C.; Weir, D. *Can. J. Chem.* **1988**, *66*, 491.

Molecular and Electronic Structure of Pyracylene

Beat Freiermuth,[‡] Stefan Gerber, Andreas Riesen,[§] Jakob Wirz,* and Margareta Zehnder[§]

Contribution from the Institut für Physikalische Chemie der Universität Basel, Klingelbergstrasse 80, CH-4056 Basel, Switzerland, and the Institut für Anorganische Chemie der Universität Basel, Spitalstrasse 51, CH-4056 Basel, Switzerland. *Received May 12, 1989*

Abstract: Pyracylene (cyclopent[*fg*]acenaphthylene, **1**) is available in two steps from pyrene and, contrary to previous experience, can be crystallized, stored as a solid, and even sublimed without decomposition. The X-ray structure of **1** exhibits a pronounced alternation of bond lengths along the 12-π periphery. The absorption spectrum (with transition moment directions) and the photoelectron spectrum of **1** are reported and analyzed. Pyracylene is quite stable to irradiation both as a solid and in solution. Radiationless deactivation of the lowest excited singlet state is very rapid; fluorescence and intersystem crossing yields were below our limits of detection ($\phi_F < 3 \times 10^{-4}$, $\phi_T < 2 \times 10^{-2}$). The lowest triplet state, observed by flash photolysis with a sensitizer ($\lambda_{max} = 360$ nm, $\epsilon > 10^4$ M^{-1} cm^{-1}; $\lambda_{max} = 520$ nm, $\epsilon = 7500$ M^{-1} cm^{-1}), is also rather short-lived ($\tau = 4.6$ μs). The triplet energy of **1** is bracketed in the range of 103 ± 20 kJ mol^{-1} on the basis of energy-transfer experiments. A major component of flame soots, which had been tentatively attributed to **1** by GC–MS analysis, is shown not to be identical with **1**. The heat of formation of **1** is calculated as $\Delta_f H = 410$ kJ mol^{-1} with the MMP2 force field.

The literature on pyracylene (cyclopent[*fg*]acenaphthylene, **1**) displays a remarkable dichotomy. On the one hand, **1** is held to be very unstable, a prototype "antiaromatic" molecule with a planar 12-π periphery. The first attempts to synthesize **1** by standard procedures have failed,[1] and when the synthesis was achieved by Trost and co-workers,[2] they found that their product

‡ This work is part of the Ph. D. thesis of B.F., University of Basel, 1987.
§ Institut für Anorganische Chemie.

(1) Anderson, A. G.; Wade, R. H. *J. Am. Chem. Soc.* **1952**, *74*, 2274.

0002-7863/90/1512-738$02.50/0

Scheme I

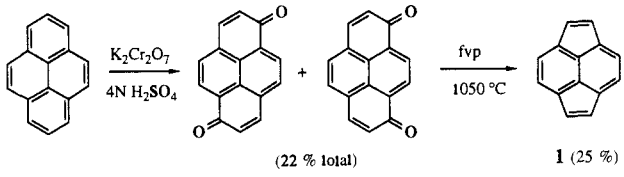

could only be stored in dilute solution; the half-life of solid **1** was reported to be on the order of a minute. The same authors have emphasized an upfield shift of ca. 1 ppm in the ^1H NMR signals of **1** as evidence for a paramagnetic ring current. In a recent theoretical paper on polycyclic hydrocarbons, the resonance energy of **1** was calculated to be by far the lowest of all molecules considered, and the possibility of a survival of this molecule in the environment was dismissed.[3a]

On the other hand, in a study concerned with thermodynamic stabilities of hydrocarbons, **1** was predicted to be the most stable hydrocarbon of composition $C_{14}H_8$ up to a temperature of 2500 K.[4] Pyracylene was repeatedly proposed to be a major component of soot resulting from the incomplete combustion of acetylene or ethylene,[5] liquid fossil fuels, wood, or coal.[6,7] It was also suggested as a likely component of interstellar clouds.[8] Finally, the carbon framework of **1** is a subunit of the spheroidal structure ascribed to C_{60} and larger carbon clusters that are formed spontaneously by laser vaporization of graphite.[9] Experimental support for the stability of **1** at high temperatures in the gas phase comes from the work of Schaden.[10] He reported that flash vacuum pyrolysis (FVP) of pyrene quinones yields **1** and has thereby provided an attractively simple two-step synthesis of **1** (Scheme I).

We have found that the reported instability of solid pyracylene is mainly due to the presence of some reactive impurities. After careful purification, the compound can be crystallized, stored, and sublimed. This has opened the way to a characterization by X-ray analysis, photoelectron spectroscopy, and electronic absorption spectroscopy.

Experimental Section

Preparation and Purification of Pyracylene (1). A mixture of pyrene-1,6-dione and pyrene-1,8-dione (2 g, 8.6 mmol), obtained by potassium dichromate oxidation of pyrene,[11] was flash pyrolyzed as described by Schaden.[10] The pyrolysate was immediately washed from the cold trap with a small amount of CH_2Cl_2 and flash chromatographed on neutral, active aluminum oxide with the same solvent. The red pyracylene fraction (R_f = 0.63) was evaporated and the residue was rapidly redissolved in petroleum ether and rechromatographed on silica gel with petroleum ether as solvent. The red-brown eluate contained 550 mg of **1**, as estimated by absorption spectroscopy.

Further purification either by repeated crystallization from pentane at −20 °C, or by chromatography with $CH_2Cl_2/CHCl_3$ on alumina which had been impregnated with silver nitrate (25 g of alumina were treated with 2.5 g of $AgNO_3$ in 50 mL of H_2O and dried at 110 °C in vacuo), gave a total yield of 374 mg of **1**. A final slow crystallization at −20 °C from a relatively dilute pentane solution gave octahedral crystals of **1** that were suitable for X-ray analysis and showed no sign of decomposition after being stored at −20 °C for many months or at room temperature for several days. The crystals decomposed without melting at 130 °C.

X-ray Data Collection. The crystal data and some details of the data collection and structure refinement are summarized in Table I. The fractional atomic coordinates and their anisotropic thermal parameters are given in Table II.

Preparation and Analysis of Soot. Fir wood (2 kg) was burnt in a freshly cleaned stove. The deposit of soot which formed on the heat exchanger was collected (300 mg), dried in vacuo, and extracted during 4 h with CH_2Cl_2 in a Soxhlet apparatus. The extract was condensed and flash chromatographed on silica with CH_2Cl_2. The red eluate was concentrated to 0.5 mL and used for gas chromatography on a 10 m × 0.32 mm capillary column coated with 5-μm methyl-5% phenyl-silicone as a stationary phase (injection volume 1.5 μL, injection temperature 300 °C, oven temperature programmed from 90 to 250 °C with a temperature gradient of 2 °C/min, detection by FID and/or MS).

Semiempirical Calculations. Predictions for electronic spectra of closed-shell species were obtained with standard PPP SCF SCI calculations[12] (carbon framework geometry from X-ray analysis; electron repulsion integrals: $\gamma_{\mu\nu}$ = 1439.5/[132.8 + $R_{\mu\nu}$/pm] eV; resonance integrals "constant": $\beta_{\mu\nu}$ = −2.318 eV, or "variable": $\beta_{\mu\nu}$ = −2.318 × exp{0.335[$p_{\mu\nu}$ − $^2/_3$]} eV, as indicated). The same parameters (constant $\beta_{\mu\nu}$) were used with the open-shell programs to calculate triplet–triplet[13] and radical ion[14] absorption spectra by the PPP SCF SCI method. MNDO

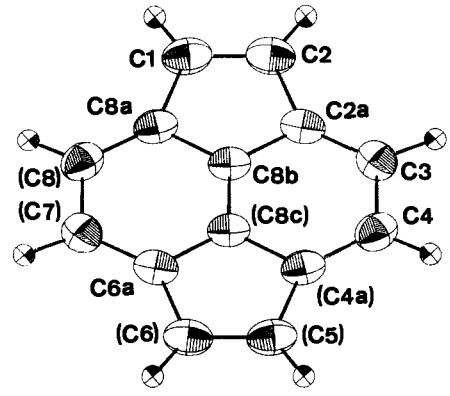

Figure 1. ORTEP stereodrawing of the molecular structure of pyracylene (**1**).

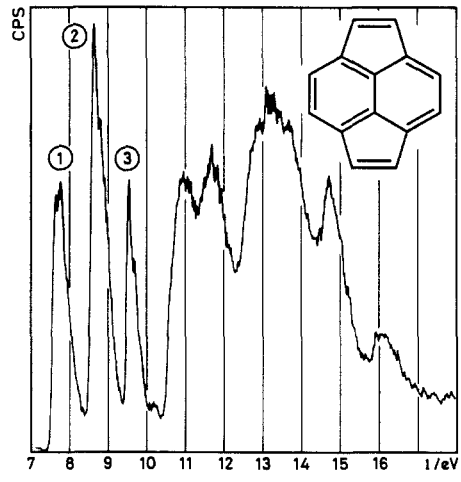

Figure 2. He I photoelectron spectrum of pyracylene (**1**).

(2) (a) Trost, B. M.; Bright, G. M. *J. Am. Chem. Soc.* **1967**, *89*, 4244. (b) Trost, B. M.; Nelsen, S. F.; Britelli, D. R. *Tetrahedron Lett.* **1967**, *40*, 3959. (c) Trost, B. M.; Bright, G. M. *J. Am. Chem. Soc.* **1968**, *90*, 2732. (d) Trost, B. M.; Bright, G. M. *Ibid.* **1969**, *91*, 3689. (e) Trost, B. M.; Bright, G. M.; Frihart, C.; Britelli, D. *Ibid.* **1971**, *93*, 737. (f) Trost, B. M. In *Topics in Nonbenzenoid Aromatic Chemistry*; Hirokawa Publ. Co.: Tokyo, 1973; Vol. I, p 243. (g) Trost, B. M.; Buhner, D.; Bright, G. M. *Tetrahedron Lett.* **1973**, *29*, 2787. (h) Trost, B. M.; Herdle, W. B. *J. Am. Chem. Soc.* **1976**, *98*, 4080.

(3) (a) Aihara, J. *Bull. Chem. Soc. Jpn.* **1988**, *61*, 1451. (b) Aihara, J.; Hosoya, H. *Ibid.* 2657.

(4) Stein, S. E.; Fahr, A. *J. Phys. Chem.* **1985**, *89*, 3714.

(5) Crittenden, B. D.; Long, R. *Environ. Sci. Technol.* **1973**, *7*, 742.

(6) Schultz, J. L.; Kessler, T.; Friedel, R. A.; Sharkey, A. G. *Fuel* **1972**, *51*, 242.

(7) (a) Laflamme, R. E.; Hites, R. A. *Geochim. Cosmochim. Acta* **1978**, *42*, 289. (b) Lee, M. L.; Prado, G. P.; Howard, J. B.; Hites, R. A. *Biomed. Mass Spectrom.* **1977**, *4*, 182. (c) Howard, J. B.; Longwell, J. P. In *Polynuclear Aromatic Hydrocarbons: Formation, Metabolism and Measurement*; Cooke, M., Dennis, A. J., Eds.; Batelle Press: Columbus, OH, 1983; p 27.

(8) Keller, R. In *Polycyclic Aromatic Hydrocarbons and Astrophysics*; Léger, A., et al., Eds.; Reidel Publ.: Dordrecht, The Netherlands, 1987; p 387.

(9) Kroto, H. W.; Heath, J. R.; O'Brien, S. C.; Curl, R. F.; Smalley, R. E. *Nature* **1985**, *318*, 162. Zhang, Q. L.; O'Brien, S. C.; Heath, J. R.; Liu, Y.; Curl, R. F.; Kroto, H. W.; Smalley, R. E. *J. Phys. Chem.* **1986**, *90*, 525. Yang, S. H.; Pettiette, C. L.; Chesnovsky, O.; Smalley, R. E. *Chem. Phys. Lett.* **1987**, *139*, 233. Heath, J. R.; Curl, R. F.; Smalley, R. E. *J. Chem. Phys.* **1987**, *87*, 4236. Kroto, H. *Science* **1988**, *242*, 1139. See also ref 3b and Mallion, R. B. *Nature* **1987**, *325*, 760.

(10) Schaden, G. *J. Org. Chem.* **1983**, *48*, 5385.

(11) Goldschmiedt, G. *Monatsh. Chem.* **1883**, *4*, 309. Fatiadi, A. J. *J. Chromatogr.* **1965**, *20*, 319. Cho, H.; Harvey, R. G. *J. Chem. Soc., Perkin Trans. 1* **1976**, 836.

(12) Pariser, R.; Parr, R. G. *J. Chem. Phys.* **1953**, *21*, 466. Pople, J. A. *Trans. Faraday Soc.* **1953**, *49*, 1375.

(13) Gisin, M.; Wirz, J. *Helv. Chim. Acta* **1983**, *66*, 1556.

Table I. Crystal Data and Parameters Used in Structure Determination

IUPAC name	cyclopent[*fg*]acenaphthylene
formula	$C_{14}H_8$
formula weight	176.1 g
space group	monoclinic, $P2_1/n$
a	7.093 (1) Å
b	9.032 (1) Å
c	7.095 (2) Å
α	90.0°
β	100.05 (15)°
γ	90.0°
V	447.56 Å^3
Z	2
calculated density	1.307 g/cm^3
radiation, wavelength	Mo Kα, 0.71069 Å
linear absorption coefficient	0.38 cm^{-1}
F(000)	184.000
crystal size	0.3 × 0.2 × 0.2 mm^3
diffractometer used	Enraf-Nonius CAD 4
method of measuring intensities	$\omega/2\theta$
number and θ range of reflections used for measuring lattice parameters	25, 10°
range of *h*, *k*, and *l*	$-8 \le h \le 8$; *k*, 0–11; *l*, 0–8
temperature during data collection	ambient
standard reflections and their intensity variation throughout experiment	4 standards monitored every 3600 s showed no significant variation
number of reflections measured	940
number of unique reflections	718
value of $R_{int}[\sum\|F - \langle F\rangle\|/\sum]$ from merging equivalent reflections	0.1196
number of unobserved reflections	150
criterion for recognizing unobserved reflections [$I < n\sigma(I)$]	$I < 3\sigma(I)$
method used to solve structure	direct
magnitudes in least-squares refinement	*F*(Sheldrick 76)
method of locating and refining H atoms	difference Fourier map
parameters refined	80
final value of *R*, R_w	0.0406, 0.0461
method used to calculate *w*	$w = 1.0411/\sigma(F)^2 + 2.77 \times 10^{-3} F^2$
$(\Delta/\sigma)_{max}$	0.036
$(\Delta\rho)_{max}$, $(\Delta\rho)_{min}$	0.125 e/Å^3, −0.171 e/Å^3
source of atomic scattering factors and *f*′ and *f*″ values	used as given in SHELX-76
computer programs used	SHELX-86,[a] SHELX-76,[b] ORTEP[c]

[a] Sheldrick, G. M., University of Göttingen, 1986. [b] Sheldrick, G. M., University of Cambridge, 1976. [c] Reference 17.

calculations were done with a 1986 edition of AMPAC by Dewar and co-workers[15] and force field calculations with the 1986 MMP2 program of Allinger.[16]

Results

X-ray Analysis of the Molecular Structure. The structure of **1** is displayed as an ORTEP[17] stereodrawing in Figure 1. The atomic coordinates (Table II) are compatible, within experimental error, with D_{2h} molecular symmetry; C–C bond lengths and C–C–C bond angles are given in Table III.

Photoelectron Spectrum. The He I photoelectron spectrum of **1** exhibits three resolved features, labeled ① to ③, with intensity maxima at 7.77, 8.65, and 9.52 eV, respectively (Figure 2). The high intensity of feature ② suggests that it arises from two overlapping ionization bands. A window of over I eV separates band ③ from the onset of the congested high-energy bands. A Hückel model, which accounts for bond lengths changes upon ionization by a simple perturbation treatment,[18] was used to correlate orbital energies with vertical ionization potentials I_v on

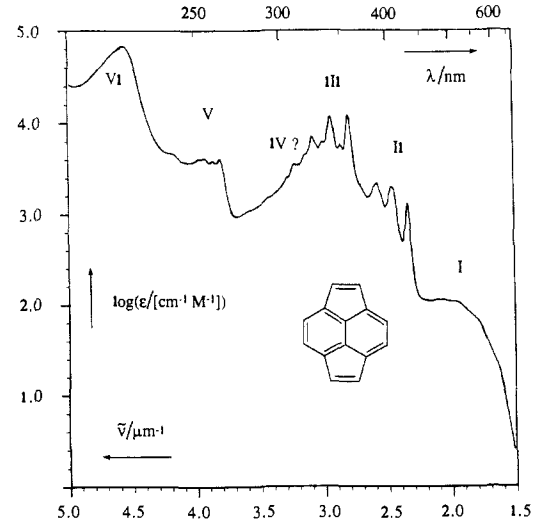

Figure 3. Electronic spectrum of pyracylene (**1**) in hexane solution at ambient temperature. Selected values of absorbance maxima $\tilde{\nu}_{max}/\mu m^{-1}$ and their intensities log (ϵ/M^{-1} cm^{-1}) are given in Table IV. The diagram was combined from three spectra of 10^{-2}, 10^{-3}, and 10^{-4} M solutions which obeyed Beer's law.

the basis of Koopmans' theorem. Using this model we predict the following values for the first five vertical π-ionization energies: $I_{v,1}(2b_{2g}) = 7.99$; $I_{v,2}(1a_u) = 8.40$; $I_{v,3}(3b_{3u}) = 8.97$; $I_{v,4}(2b_{3u}) = 9.41$, and $I_{v,5}(1b_{1g}) = 11.14$ eV (the symmetry labels refer to Cartesian coordinates with the *y* and *z* axes in the molecular plane, *z* parallel to the central bridging bond). On this basis we attribute feature ① to ionization from the $2b_{2g}$ orbital, feature ② to orbitals $1a_u$ and $3b_{3u}$, and feature ③ to orbital $2b_{3u}$.

Absorption Spectrum and Linear Dichroism. The electronic spectrum of **1** has hitherto been characterized only by the quotation of λ_{max} values;[2a,c,e,f] extinction coefficients were not given. The absorption spectrum of an analytical sample of **1** in hexane solution at ambient temperature is shown in Figure 3. The vibrational fine structure was somewhat more pronounced in an absorption spectrum recorded with a glassy alkane solution of **1** at 77 K, but the S_0–S_1 absorption band remained diffuse.

The transition moment directions were determined from the linear dichroism of stretched polyethylene sheets which had been doped with **1** and cooled to 77 K. The dichroic absorption curves $E_\parallel(\lambda)$ and $E_\perp(\lambda)$ were measured with calcite Glan prism polarizers with their electric vector set parallel and orthogonal to the stretching direction, respectively. The two spectra were analyzed by the method of stepwise reduction due to Thulstrup, Eggers, and Michl (TEM model)[19] to give orientation factors $K_z = 0.57$ and $K_y = 0.33$. These values conform well with expectations based on the molecular shape of **1** (ratio of the molecular diameters $d_y/d_z = 1.14$, where d_y and d_z are the distances between the peripheral H atoms determined by X-ray analysis, Table II). The orientation factors reported for pyrene (0.54 and 0.32),[20] a molecule of similar shape, are practically identical.

Experimental band maxima and polarizations are summarized in Table IV, together with the results of standard PPP SCF SCI calculations.[12] Similar calculations have been published previously.[21-23] These calculations unanimously predict two bands of comparable intensity but different polarization (B_{1u} and B_{2u}) in the spectral range $2.6 < \tilde{\nu}/\mu m^{-1} < 3.3$. This is not born out by the polarization measurements, however; practically all of the

(14) Zahradnik, R.; Čársky, P. *J. Phys. Chem.* **1970**, *74*, 1235.
(15) AMPAC QCPE 506, version 1.0, 1986.
(16) Allinger, N. L., QCPE program MMP2, 1986.
(17) Johnson, C. K., ORTEP. Report ORNL-5138, Oak Ridge National Laboratory: Oak Ridge, TN, 1976.
(18) Brogli, F.; Heilbronner, E. *Theor. Chim. Acta* **1972**, *26*, 290.
(19) Thulstrup, E. W.; Michl, J. *J. Am. Chem. Soc.* **1982**, *104*, 5594. Michl, J.; Thulstrup, E. W. *Spectroscopy with Polarized Light*; VCH Publishers: New York, 1986.
(20) Thulstrup, E. W.; Downing, J. W.; Michl, J. *Chem. Phys.* **1977**, *23*, 307.
(21) Yamaguchi, H.; Nakajima, T. *Bull. Chem. Soc. Jpn.* **1971**, *44*, 682; *Pure Appl. Chem.* **1971**, *28*, 219.
(22) DasGupta, N. K.; Birss, F. W. *Bull. Chem. Soc. Jpn.* **1978**, *51*, 1211.
(23) Favini, G.; Gamba, A.; Simonetta, M. *Theor. Chim. Acta* **1969**, *13*, 175.

Table II. Fractional Atomic Coordinates and Their Anisotropic Thermal Parameters $U_{i,i}$ (10^{-4} Å^2)

atom[a]	x/a	y/b	z/c	U_{11}	U_{22}	U_{33}	U_{23}	U_{13}	U_{12}
C(1)	0.8127 (3)	0.3125 (2)	0.6889 (3)	596 (13)	445 (12)	466 (10)	−72 (10)	−52 (11)	−33 (10)
C(2)	0.6890 (3)	0.3126 (2)	0.8128 (3)	467 (11)	451 (12)	551 (12)	−22 (10)	−53 (10)	−64 (9)
C(2a)	0.7661 (3)	0.4055 (2)	0.9830 (3)	395 (10)	383 (10)	479 (11)	27 (8)	−23 (8)	−2 (8)
C(3)	0.7196 (3)	0.4519 (2)	1.1541 (3)	413 (10)	457 (12)	530 (12)	68 (9)	64 (9)	5 (8)
C(4)	0.8460 (3)	0.5481 (2)	1.2804 (3)	547 (12)	459 (12)	417 (10)	12 (9)	51 (9)	71 (9)
C(8a)	0.9827 (3)	0.4050 (2)	0.7660 (3)	481 (11)	377 (11)	400 (10)	−2 (8)	−27 (8)	35 (8)
C(8b)	0.9401 (3)	0.4549 (2)	0.9403 (3)	416 (9)	358 (10)	403 (9)	10 (7)	−20 (7)	17 (7)
H(1)	0.7893 (30)	0.2662 (26)	0.5657 (33)	634 (65)					
H(2)	0.5629 (35)	0.2561 (26)	0.7955 (31)	694 (69)					
H(3)	0.6003 (32)	0.4180 (23)	1.1995 (29)	500 (53)					
H(4)	0.8015 (32)	0.5762 (24)	0.3984 (35)	617 (62)					

[a] See Figure 1 for numbering of centers.

Table III. Bond Lengths and Bond Angles of **1**[a]

	bond length/pm			degrees	
bond	obsd	calcd[b]	bond angle	obsd	calcd[b]
C(1)–C(2)	134.6 (3)	137.0	C(1)–C(2)–C(2a)	109.8 (2)	110.3
C(2)–C(2a)	149.2 (3)	146.8	C(1)–C(8a)–C(8b)	102.7 (2)	101.5
C(2a)–C(3)	137.9 (3)	138.7	C(2a)–C(3)–C(4)	120.9 (2)	120.4
C(2a)–C(8b)	139.7 (3)	140.4	C(2a)–C(8b)–C(8a)	115.1 (2)	116.5
C(3)–C(4)	144.3 (3)	144.1	C(2a)–C(8b)–C(8c)	122.5 (2)	121.8
C(8b)–C(8c)	136.0 (3)	136.9	C(3)–C(2a)–C(8b)	116.7 (2)	117.8

[a] Deviations of the atomic coordinates (Table II) from D_{2h} molecular symmetry are within the experimental standard deviations. The molecular parameters given in this table were obtained as arithmetic means of experimental values which are equivalent under assumed D_{2h} molecular symmetry. [b] Results of MMP2 calculation;[16] convergence to D_{2h} symmetry was reached without imposing symmetry restrictions.

intensity and vibrational fine structure appears in the reduced spectrum $A_{\parallel}(\lambda)$, while $A_{\perp}(\lambda)$ exhibits only a weak hump with hardly any fine structure in that region (Figure 4). Apart from this unresolved discrepancy, all calculations agree satisfactorily with the experimental spectrum.

Photochemical and Photophysical Properties, the Triplet State. Pyracylene, as a solid as well as in degassed or aerated solution, was remarkably resistant to photolysis by unfiltered light from a 150-W high-pressure mercury arc. Although a systematic study was not performed, **1** appeared to be one of the most photostable organic chromophores we have had occasion to irradiate.

Flash photolysis of pyracylene in hexane or acetonitrile solution either at 530 nm (Nd glass laser, 200 mJ, 20 ns) or at 248 nm (KrF excimer laser, 200 mJ, 25 ns) gave no detectable transient absorption. However, it was possible to generate and observe the triplet state of pyracylene (^{3}**1**) by energy transfer using benzophenone as a sensitizer. Excitation at 248 nm of degassed acetonitrile solutions containing both benzophenone (ca. 3×10^{-5} M) and pyracylene (up to 2×10^{-4} M) gave biphasic decay curves. The rate of the fast process was proportional to the concentration of **1**, giving an energy-transfer rate constant of ca. 1.2×10^{10} M^{-1} s^{-1}. The slower process, $k_d \cong 2.2 \times 10^5$ s^{-1}, is attributed to the radiationless decay of ^{3}**1**. The absorption of ^{3}**1** extends up to 600 nm (λ_{max} = 520 nm). Throughout most of the visible region the energy-transfer process was seen as a decay rather than as a grow-in of absorption. At these wavelengths, the extinction coefficient of ^{3}**1** is lower than that of triplet benzophenone. Around 520 nm, the transient decay curves fitted quite well to a single exponential. Hence the extinction coefficients of ^{3}**1** and triplet benzophenone must be nearly equal at this wavelength which nearly coincides with the broad absorption maximum of triplet benzophenone, $\epsilon = (7.5 \pm 1.0) \times 10^3$ M^{-1} cm^{-1}.[24] Around 360 nm the energy-transfer process was observed as a grow-in of absorbance. This indicates that ^{3}**1** has a stronger absorption maximum at ca. 360 nm with an extinction coefficient well over 10^4 M^{-1} cm^{-1}. The results of open-shell PPP SCF SCI calculations[13] agree well with these experimental findings; several rather weak triplet–triplet absorption bands are predicted to lie in the visible region and a very strong band in the near-UV: λ_{max} (oscillator strength f) 326 (1.66), 415 (0.16), 536 (0.02), 575 (0.03), 1025 (0.07), and 1113 nm (0.01).

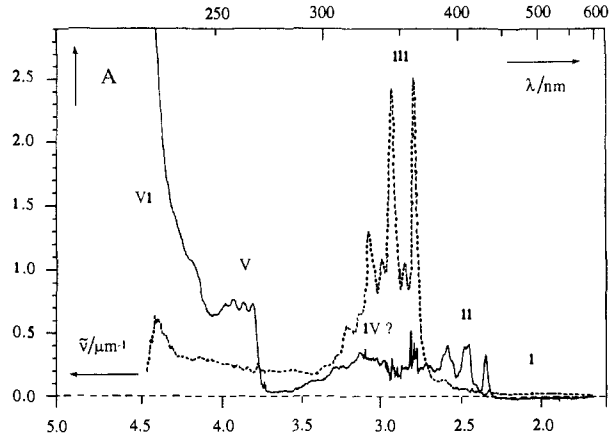

Figure 4. Reduced dichroic absorption spectra of pyracylene (**1**) oriented in a stretched polyethylene sheet at 77 K (dotted line, orthogonal; full line, parallel to the stretching direction).

Further energy-transfer experiments were performed in order to bracket the triplet energy of **1**: triplet tetracene (E_T = 123 kJ mol^{-1})[25] was quenched at a diffusion-controlled rate by **1**, whereas quenching of triplet pentacene ($E_T \cong 83$ kJ mol^{-1})[26] could not be detected, $k_q < 2 \times 10^6$ M^{-1} s^{-1}.

Redox Properties. When a degassed solution of **1** in dry tetrahydrofuran (THF) was brought in contact with a potassium mirror, a bright orange color immediately developed due to the formation of pyracylene radical anion (**1**$^{\bullet-}$). Spectra taken from partly reduced solutions exhibited isosbestic points at 305 and 368 nm which were used to estimate absolute extinction coefficients for **1**$^{\bullet-}$. The concentration of **1**$^{\bullet-}$ reached its maximum when the solution had been exposed to the potassium mirror for about 30 s. Such solutions gave rise to a strong ESR spectrum of **1**$^{\bullet-}$ (two sets of four equivalent protons with coupling constants of 25 and 19 mT, respectively) as reported by Trost et al.[2b] The absorption spectrum of **1**$^{\bullet-}$ {λ_{max}/nm (log [ϵ/M^{-1} cm^{-1}])} 284 (3.8), 440 (4.10), 449 (4.09), 486 (3.90), 522 (3.37), and 542 (3.51)} was in satisfactory agreement with predictions from PPP SCF SCI calculations[14] {λ_{max}/nm (oscillator strength f) 262 (0.30), 440 (0.04), 454 (0.31), 535 (0.002), 545 (0.01), 1391 (0.00)}. Upon further reduction, a secondary product with λ_{max} = 383 nm, log (ϵ/M^{-1} cm^{-1}) = 4.0, weak shoulder extending to 500 nm, formed slowly. This is attributed to pyracylene dianion (**1**$^{2-}$), PPP SCF SCI calculations[12] for **1**$^{2-}$ gave {λ_{max}/nm (oscillator strength f) 303 (0.2), 368 (0.6), and 426 (0.00)}. Attempts to generate and characterize the radical cation of **1** by ESR spectroscopy have failed. As expected from the low value of the first ionization potential, $K_{v,1}$(**1**) = 7.77 eV, pyracylene reacted rapidly with oxidizing agents such as aluminum chloride or tris(*p*-bromophenyl)aminyl hexachloroantimonate in methylene chloride, but

(24) Carmichael, I.; Hug, G. L. *J. Phys. Chem. Ref. Data* **1986**, *15*, 1.

(25) Birks, J. B. *Photophysics of Aromatic Molecules*; Wiley-Interscience: New York, 1970.

(26) Burgos, J.; Pope, M.; Swenberg, C. E.; Alfano, R. R. *Phys. Status Solidi B* **1977**, *83*, 249.

Table IV. Experimental and Predicted Electronic Absorption Spectrum of 1

experimental (hexane solution, 298 K)			calculated (PPP SCF SCI)		
				$\tilde{\nu}/\mu m^{-1}$ (f)[c]	
$\tilde{\nu}_{max}/\mu m^{-1}$	log (ϵ/M^{-1} cm^{-1})	polarization[a] (band no.)[b]	symm label	constant $\beta_{\mu\nu}$	variable $\beta_{\mu\nu}$
2.066	2.05	– (I)	B_{3g}	1.31 (0)	1.84 (0)
2.336	3.12				
2.463	3.29	y (II)	B_{2u}	2.33 (0.02)	2.59 (0.05)
2.577	3.33				
2.793	4.08				
2.857	3.76	z (III)	B_{1u}	2.81 (0.36)	2.98 (0.33)
2.933	4.07				
3.077	3.84				
3.125	3.65	y? (IV)	B_{2u}	2.97 (0.25)	3.27 (0.16)
3.802	3.59	y (V)	B_{2u}	4.07 (0.25)	4.28 (0.0001)
3.922	3.62				
4.546	4.84	y (VI)	B_{2u}	4.71 (1.80)	4.70 (2.08)

[a] Determined with stretched polyethylene sheets (Figure 4). [b] As shown in Figure 3. [c] Calculated oscillator strength f; for details of calculation see the Experimental Section.

such solutions failed to give ESR signals.

Is Pyracylene a Major Component of Soot? A soot extract obtained from burning fir wood gave a gas chromatogram with much the same pattern as that reported by Hites and co-workers.[7b] A number of predominant peaks were analyzed by mass spectrometry. The retention times were linearly related to those given by Hites, our times being 20% longer. In particular, we have also observed their "peak nr. 10" of mass m/z = 176 (176.059)[5] with similar intensity. As noted previously,[7b] this peak probably arises from two compounds with very similar retention times; in addition to the mass peak attributed to $C_{14}H_8$ there was a strong signal at m/z = 168, possibly due to dibenzofuran. Coinjected authentic pyracylene (**1**) was eluted with a retention time of 43.7 min, where the original gas chromatogram was essentially empty, clearly separated from "peak nr. 10", which, in our case, had a retention time of 39.4 min. This proves that "peak nr. 10" must arise from a compound or compounds other than **1**. Our result does not entirely rule out that **1** is formed in soot, however, because it may have reacted with other components during deposition or workup. A soot sample prepared similarly by burning kerosene did in fact contain a minor peak which coincided exactly with that of authentic **1** in the GC. However, this weak peak was poorly separated from stronger signals and therefore was not investigated any further.

Discussion

The ^{1}H NMR signals of pyracylene (**1**) appear at relatively high field (δ = 6.0 and 6.5 ppm),[2f] indicating some paramagnetic ring current,[27] but the high-field shift of ca. 1 ppm is moderate when compared with that of other bridged [4n]annulenes such as cycl[3.3.3]azine (**2**) (δ = 1.9 and 3.4 ppm),[28] trisdehydro[12]annulene (**3**) (4.4 ppm),[29] 8b,8c-diazapyracylene (**4**) (ca. 5.2 ppm),[30] or dipleiadiene (**5**) (ca. 4.6 ppm).[31] Comparison with available reference compounds[32] indicates that the upfield shifts of some 4 ppm in **2** and 3 ppm in **3** arise predominantly from a paramagnetic ring current rather than from the presence of a heteroatom in **2** or from anisotropies of the acetylenic groups in **3**.

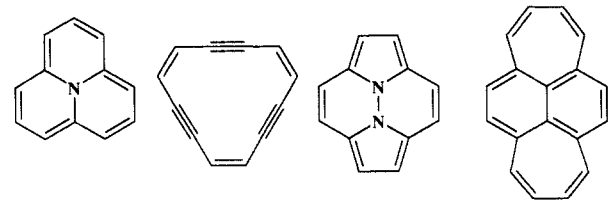

2 3 4 5

Pyracylene (**1**) has been dubbed a prototype "perturbed [12]annulene"; it was expected that the bridging central double bond should exert only a minimal perturbing effect upon the 12-π periphery of the ring system and that the steric constraints should reduce the ability of the molecule to relieve unfavorable electronic interactions by bond alternation.[2f] The X-ray structure of **1** (Figure 1, Tables I–III) reveals that the molecule is essentially planar but that it exhibits quite pronounced bond-length alternation along the molecular periphery. Perhaps most striking is the fact that bond fixation in the fused cyclopentene moieties of pyracylene (C1–C2, 134.6; C2–C2a, 149.2 pm) is significantly *enhanced* relative to that in acenaphthylene (**6**, C1–C2, 139.5; C2–C2a, 146.6 pm).[35] On the basis of simple resonance theory (Pauling structure count), one would have expected just the opposite behavior: in addition to the three resonance structures **1a–c**,

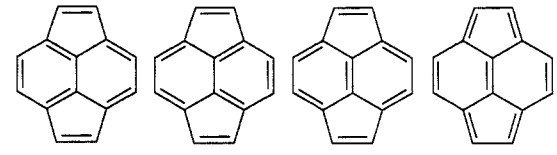

1a **1b** **1c** **1d**

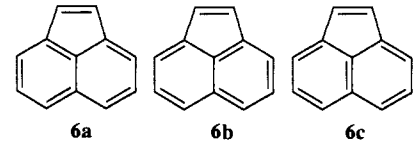

6a **6b** **6c**

which have their analogues in the case of acenaphthylene (**6a–c**), an additional structure **1d** can be drawn for pyracylene. It appears that the structure **1d** contributes negatively to the structure count

(27) Coulson, C. A.; Mallion, R. B. *J. Am. Chem. Soc.* **1976**, *98*, 592. Gomes, J. A. N. F.; Mallion, R. B. *J. Org. Chem.* **1981**, *46*, 719.
(28) Farquhar, D.; Gough, T. T.; Leaver, D. *J. Chem. Soc., Perkin Trans. 1* **1976**, 341.
(29) (a) Sondheimer, F. *Acc. Chem. Res.* **1972**, *5*, 81. (b) Gygax, R.; Wirz, J.; Sprague, J. T.; Allinger, N. L. *Helv. Chim. Acta* **1977**, *60*, 2522.
(30) Atwood, J. L.; Hrncir, D. C.; Wong, C.; Paudler, W. W. *J. Am. Chem. Soc.* **1974**, *96*, 6132.
(31) Vogel, E.; Neumann, B.; Klug, W.; Schmickler, H.; Lex, J. *Angew. Chem.* **1985**, *97*, 1044; *Angew. Chem., Int. Ed. Engl.* **1985**, *24*, 1046.
(32) (a) The ^{1}H NMR chemical shifts of **2** are among the highest reported for hydrogen atoms bonded to olefinic carbon. The triplet energy of cycl[3.3.3]azines is strongly raised upon substitution of acceptor groups (aza nitrogen for CH, ester or cyano groups for H) at the 1-, 3-, ... position(s),[33] and concomitantly, all peripheral hydrogens are deshielded by several ppm, including those at positions remote from the substituents. E.g., the substitution of ethyl ester groups at positions 1 and 3 of **2** results in a 3.2 ppm downfield shift of the signals of H_6 and H_7,[28] 1,3,6-triaza substitution of **2** gives rise to a 3.1 ppm downfield shift of H_8,[34a] and 1,6-diaza substitution of **2** to a 2.5 ppm downfield shift of H_8.[34b] (b) The chemical shifts observed for the exocyclic protons in 1,5-bisdehydro[12]annulene are similar to that of **3**, including protons which are fairly remote from the acetylenic moieties; the endocyclic proton of 1,5-bisdehydro[12]annulene is shifted *downfield* to ca. 17.6 ppm![29b]

(33) Leupin, W.; Wirz, J. *J. Am. Chem. Soc.* **1980**, *102*, 6068.
(34) (a) Ceder, O.; Vernmark, K. *Acta Chem. Scand.* **1973**, *27*, 3259. (b) Gotou, H.; Kurata, K.; Tominaga, Y.; Matsuda, Y. *J. Org. Chem.* **1985**, *50*, 4028.
(35) Wood, R. A.; Welberry, T. R.; Rae, A. D. *J. Chem. Soc., Perkin Trans. 2* **1985**, 451.

as suggested by the theory of Herndon.[36]

The geometry of **1** has been predicted in several theoretical papers.[21,22,37,38] All of these are based on semiempirical SCF calculations for the π-electron distribution, and the bond lengths are predicted on the basis of calculated bond orders. Not surprisingly, all of these calculations are highly correlated with each other and indeed with simple HMO bond orders for **1** (correlation coefficient $r > 0.96$). However, all of these models give rather poor predictions for the bond lengths with rms deviations of 3.1 pm ($r \cong 0.6$). We have thus performed MMP2[16] force field and MNDO[15] calculations, both of which take account of the σ-framework in an appropriate manner. These calculations gave significantly better results, particularly the former (Table III, rms error 1.5 pm).

Comparison with the structure of 8b,8c-diazapyracylene (**4**), reported by Paudler and co-workers,[30] is difficult, because this compound deviates considerably from D_{2h} symmetry. Nevertheless it is clear that the bond-length alternation in the diaza derivative **4**, where all bond lengths along the periphery are within 140 ± 3 pm, is much less pronounced than in the hydrocarbon **1**. The bond lengths in the naphthalenic core of **1** are quite different from the same substructure in dipleiadiene (**5**), a vinyl cross-linked [16]annulene.[31]

Experimental data for the heat of formation of **1** are not available but are now within reach, since **1** can be isolated in pure form. A simple additivity scheme based on Benson's increments and an experimental value for acenaphthylene, $\Delta_f H$(**6**, g, 298 K) = 258 ± 7 kJ mol^{-1},[39] was used by Stein and Fahr[4] to obtain an estimate of $\Delta_f H$(**1**, g, 298 K) = 366 kJ mol^{-1}. However, such a scheme completely ignores unfavorable long-range resonance effects. The heats of formation of **1** predicted by MNDO[15] and MMP2[16] are significantly higher, 461 and 410 kJ mol^{-1}, respectively. The predictions for $\Delta_f H$(**6**, g, 298 K) by these methods are 282 and 257 kJ mol^{-1}, respectively. Note the excellent agreement of the MMP2 method which also gave the best predictions for the bond lengths of **1** (vide supra). Hence we feel that the value of $\Delta_f H$(**1**, g, 298 K) = 410 kJ mol^{-1}, predicted by the latter model, is the best estimate available at present. The resonance energy calculated by Aihara[3] appears to be misleading as a guideline to estimate the thermodynamic or kinetic stability of **1**, perhaps because the method completely ignores the effects of the σ-core and of bond localization. In view of the wide discrepancy between these theoretical predictions, it would be of considerable interest to obtain an experimental value.

The abundance of polycyclic aromatic hydrocarbons increases with proximity to urban centers, and the relative abundance of specific structures in sediments is remarkably constant throughout the world. Hence the combustion of fossil fuels is considered to be the main source of aromatic hydrocarbons in the environment.[7a] Acenaphthylene (**6**) is a ubiquitous component in soots and sediments; therefore, pyracylene (**1**) was considered as the most likely structure of another widespread but unidentified constituent of composition $C_{14}H_8$.[5-7] With the authentic compound at hand, we were able to establish that the GC retention time of **1** differs considerably from this major $C_{14}H_8$ component which remains to be identified. A different, very minor constituent which we detected in a kerosene soot sample might be due to the presence of **1** in trace quantities.

Pyracylene (**1**) is very easily reduced. Trost et al. have reported two polarographic half-wave reduction potentials of −1.056 and −1.635 V vs SCE[2f] and have characterized the radical anion by ESR,[2b] the dianion by ^{1}H NMR spectroscopy.[2g] The electronic

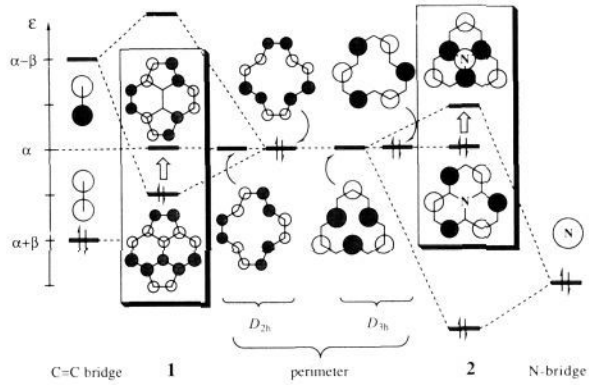

Figure 5. Frontier orbitals of **1** and **2** derived by first-order perturbation to account for the interaction of the bridge (double bond in **1**, N atom in **2**) with the nonbonding orbitals of the 12-π perimeter.

absorption spectra of these species were determined in this work. Surprisingly, our attempts to obtain evidence for the formation charge transfer complexes of **1** with electron donors have failed; no color changes or chemical reactions were observed even in quite concentrated mixtures of **1** with *p*-phenylenediamine or tetrathiofulvalene in ethanol, carbon tetrachloride, or acetonitrile as solvents.

The photophysical properties of **1** were examined by the method of flash photolysis. Energy-transfer experiments using triplet benzophenone as a sensitizer have provided a reliable estimate for the maximal extinction coefficient of triplet pyracylene (^{3}**1**) in the visible region, ϵ (520 nm) = (7.5 ± 1.5) × 10^3 M^{-1} cm^{-1}. An upper limit for the quantum yield of spontaneous $S_1 \rightarrow T_1$ intersystem crossing, ϕ_T, may be derived from the fact that no triplet absorption was detected after direct excitation of **1**; a conservative consideration of the instrumental sensitivity leads to $\phi_T < 0.02$. The lifetime of ^{3}**1** in degassed solution is $\tau_T = 4.6$ μs. Fluorescence emission of **1** is below our detection limits, even with pulsed laser excitation, $\phi_F < 3 \times 10^{-4}$. These observations are in line with previous experience,[41] namely that radiationless deactivation of the lowest singlet and triplet state is much faster in conjugated hydrocarbons containing a 4*n*-membered ring than it is in benzenoid hydrocarbons. The remarkable photostability of **1** may be attributed to the rapid radiationless deactivation of its excited states.

Pyracylene (**1**) and cycl[3.3.3]azine (**2**) can both be regarded as 12-π perimeters which are held planar by a central bridge containing two π electrons. Yet their chemical and photophysical properties are fundamentally different. Trost et al. have already pointed out that the periphery model is very much influenced by the connectivity of the cross-link.[2e] It is instructive to interpret these differences in terms of a simple frontier orbital perturbation treatment in which only the interaction of the two nonbonding perimeter orbitals with the π orbitals of the central bridging group are considered (Figure 5). Note that the starting linear combination of the two degenerate nonbonding perimeter orbitals is chosen differently for the two compounds, in accord with the reduced symmetry of each perturbation (the symmetry reduction from D_{12h} to D_{2h} for **1** and D_{3h} for **2** is already inherent in the different shapes of the carbon perimeters, but this has no bearing on the Hückel approximation). With this choice of the perimeter orbitals, only one interaction with the bridge needs to be considered in each case for reasons of symmetry. In **1**, the bonding interaction of one of the perimeter orbitals with the antibonding bridge orbital leads to a stabilization of the HOMO of **1** by 0.46 β. In the case of **2**, the LUMO is derived from the antibonding interaction of one of the perimeter orbitals with the nitrogen lone pair (*ca.* 0.48 β, the exact amount depends on the choice of heteroparameters).[33]

(36) Herndon, W. C. *J. Am. Chem. Soc.* **1974**, *96*, 7605.
(37) Lo, D. H.; Whitehead, M. A. *J. Chem. Soc., Chem. Commun.* **1968**, 771.
(38) DasGupta, A.; DasGupta, N. K. *Can. J. Chem.* **1976**, *54*, 3227.
(39) Cox, J. D.; Pilcher, G. *Thermochemistry of Organic & Organometallic Compounds*; Academic Press: London, 1970.
(40) (a) Gerson, F.; Jachimowicz, J.; Leaver, D. *J. Am. Chem. Soc.* **1973**, *95*, 6702. (b) Reference 33. (c) Leupin, W.; Berens, S. J.; Magde, D.; Wirz, J. *J. Phys. Chem.* **1984**, *88*, 1376. (d) Leupin, W.; Magde, D.; Persy, G.; Wirz, J. *J. Am. Chem. Soc.* **1986**, *108*, 17.
(41) Wirz, J. *Jerusalem Symp. Quantum Chem. Biochem.* **1977**, *10*, 283. Wirz, J.; Krebs, A.; Schmalstieg, H.; Angliker, H. *Angew. Chem.* **1981**, *93*, 192; *Angew Chem., Int. Ed. Engl.* **1981**, *20*, 192. Elsaesser, T.; Lärmer, F.; Kaiser, W.; Dick, B.; Niemeyer, M.; Lüttke, W. *Chem. Phys.* **1988**, *126*, 405.

Thus the frontier orbitals of both compounds are derived from the perimeter orbitals, but in **1** the unperturbed nonbonding perimeter orbital is the LUMO and in **2** it is the HOMO. As an immediate consequence, **1** is easily reduced and **2** is easily oxidized.

Although the HOMO–LUMO splittings in **1** and **2** are comparable in magnitude, the changes in the electronic structure arising from the perturbation are basically different in nature. In the case of **2**, the HOMO is nonbonding between *all* adjacent C atoms of the periphery, and hence, the perturbation does not favor bond-length alternation. Moreover, the HOMO is entirely localized to those centers where the LUMO has a node (Figure 5); hence, excitation to S_1 or T_1 entails a profound redistribution of charge within the molecule. The consequences [exchange integral $K_{HO,LU} \cong 0$, unusually long wavelength S_0–S_1 absorption ($\lambda_{00} \cong 1300$ nm), very small singlet triplet splitting (possibly $E_{T_1} > E_{S_1}$ in violation of Hund's rule), high sensitivity to inductive perturbation] have been discussed previously.[40] In contrast, the HOMO in **1** is alternatingly bonding and antibonding along the periphery; hence, the perturbation promotes bond-length alternation. HOMO–LUMO excitation in **1** entails some charge transfer from the bridging double bond to the periphery but little charge reshuffling on the periphery. As a consequence, the S_0–S_1 transition of **1** occurs at a much shorter wavelength ($\lambda_{00} \cong 650$ nm; $E_{S_1} \cong 184$ kJ mol^{-1}), the singlet–triplet splitting assumes a normal value ($E_{T_1} \cong 103 \pm 20$ kJ mol^{-1} from energy-transfer experiments; hence $E_{S_1} - E_{T_1} \cong 81 \pm 20$ kJ mol^{-1}), and the S_0–S_1 transition energy is not expected to be very sensitive to inductive perturbation.

Apart from numerous theoretical papers dealing with pyracylene (**1**),[21-23,27,37,38] all of the previous experimental work was performed some 15 years ago by Trost and co-workers[2] who achieved the first synthesis and provided extensive characterization of this remarkable hydrocarbon. The simple two-step synthesis (Scheme I) of **1** reported 6 years ago by Schaden[10] has not to our knowledge been exploited prior to this work. It does involve some laborious purification and gives only a modest 5% overall yield of **1**. Nevertheless, it provides relatively easy access to **1** in up to gram quantities and, as the present work shows, in storeable form. The presence of two reactive double bonds in pyracylene invites the design of various novel compounds. Some such synthetic applications are currently being explored in our laboratories.[42]

Acknowledgment. This work was performed as part of project No. 2.835-0.88 of the Swiss National Science Foundation. We thank Dr. E. Flury, Ingenieurschule beider Basel, for providing a sample of the pyrenequinone mixture. Financial support by Ciba-Geigy, SA, Hoffmann-La Roche & Cie. SA, Sandoz SA, and the Ciba Stiftung is gratefully acknowledged.

Registry No. 1, 187-78-0; pyrene-1,6-dione, 1785-51-9; pyrene-1,8-dione, 2304-85-0.

(42) Soliva, A., Diplomarbeit Universität Basel, 1988.

A Laser Flash Photolysis Study of Carbonyl Ylides of Arylchlorocarbenes: Kinetics and Reversibility of the Formation, Cyclization, and Cycloaddition

Roland Bonneau and Michael T. H. Liu*,†

Contribution from the Laboratoire de Chimie Physique A, UA 348 du CNRS, Université de Bordeaux I, 33405 Talence, France. *Received May 31, 1989*

Abstract: Carbonyl ylides formed from (*p*-nitrophenyl)chlorocarbene or phenylchlorocarbene and acetone or benzaldehyde have been studied by laser flash photolysis. The rate constants for the formation of these ylides, for their cyclization to oxiranes, and for some addition reactions have been measured. Electron-withdrawing substituents on the carbene increase the rate of ylide formation and decrease the rate of cyclization. The trapping of carbonyl ylide by para-substituted benzaldehydes gave a Hammett's ρ value equal to +1.0. The dual role of benzaldehyde, first as a constituent of the ylide and second as a trapping agent, has been demonstrated. Kinetic analysis indicates that an equilibrium exists between the phenylchlorocarbene, the acetone, and the corresponding ylide, with an equilibrium constant around 0.27 M^{-1} at 300 K.

The chemistry of carbonyl ylides has been studied extensively.[1-3] Carbonyl ylides can be generated from the photolysis of oxiranes[4] and oxadiazolines[5] or from the reaction of 1-naphthylcarbene,[6] fluorenylidene,[7] and para-substituted phenylchlorocarbenes with acetone.[8-10] Also, carbonyl ylides have been generated from aldehydes and carbenes.[11] We now report a laser flash photolysis (LFP) study of phenylchlorocarbene and (*p*-nitrophenyl)chlorocarbene with acetone or benzaldehyde to give carbonyl ylides. The ylides formed in this way collapse to give oxirane or can be trapped by benzaldehydes. Rate constants for these processes are measured.

Experimental Section

3-Chloro-3-(*p*-nitrophenyl)diazirine (**1a**) and 3-chloro-3-phenyldiazirine (**1b**) were synthesized by the oxidation of the corresponding benzamidine hydrochloride in freshly prepared sodium hypochlorite in DMSO.[12] Products of ylide cyclization and benzaldehyde addition for **1a** have been reported previously.[13]

† On leave from University of Prince Edward Island, Charlottetown, PEI, Canada.

(1) Huisgen, R. *Angew. Chem., Int. Ed. Engl.* **1977**, *16*, 572.
(2) Gill, H. S.; Landgrebe, J. A. *J. Org. Chem.* **1983**, *48*, 1051.
(3) Martin, C. W.; Landgrebe, J. A. *J. Org. Chem.* **1985**, *50*, 2050.
(4) Trozzolo, A. M.; Leslie, T. M.; Sarpotdar, R. D.; Small, R. D.; Ferraudi, G. J. *Pure Appl. Chem.* **1979**, *51*, 261.
(5) Shimizu, N.; Bartlett, P. D. *J. Am. Chem. Soc.* **1978**, *100*, 4260. Bekhazi, M.; Warkentin, J. *J. Am. Chem. Soc.* **1981**, *103*, 2473.
(6) Barcus, R. L.; Hadel, L. M.; Johnston, L. J.; Platz, M. S.; Savino, T. G.; Scaiano, J. C. *J. Am. Chem. Soc.* **1986**, *108*, 3928.
(7) Wong, P. C.; Griller, D.; Scaiano, J. C. *J. Am. Chem. Soc.* **1982**, *104*, 6631.
(8) Soundararajan, N.; Jackson, J. E.; Platz, M. S.; Liu, M. T. H. *Tetrahedron Lett.* **1988**, *29*, 3419.
(9) Ibata, T.; Liu, M. T. H.; Toyoda, J. *Tetrahedron Lett.* **1986**, *27*, 4383.
(10) Liu, M. T. H.; Soudararajan, N.; Anand, S. M.; Ibata, T. *Tetrahedron Lett.* **1987**, *28*, 1011.
(11) de March, P.; Huisgen, R. *J. Am. Chem. Soc.* **1982**, *104*, 4952. Huisgen, R.; de March, P. *J. Am. Chem. Soc.* **1982**, *104*, 4953.
(12) Graham, W. H. *J. Am. Chem. Soc.* **1965**, *87*, 4396.
(13) Ibata, T.; Toyoda, J.; Liu, M. T. H. *Chem. Lett.* **1987**, 2135.

0002-7863/90/1512-744$02.50/0